



OPEN

Dectin-1 ligands produce distinct training phenotypes in human monocytes through differential activation of signaling networks

Quen J. Cheng^{1,2}, Kylie Farrell^{1,3}, Jeffrey Fenn³, Zuchao Ma⁴, Sara K. Makanani^{2,3} & Jonathan Siemsen³

Cells of the innate immune system retain memory of prior exposures through a process known as innate immune training. β -glucan, a Dectin-1 ligand purified from the *Candida albicans* cell wall, has been one of the most widely utilized ligands for inducing innate immune training. However, many Dectin-1 ligands exist, and it is not known whether these all produce the same phenotype. Using a well-established in vitro model of innate immune training, we compared two commercially available Dectin-1 agonists, zymosan and depleted zymosan, with the gold standard β -glucan in the literature. We found that depleted zymosan, a β -glucan purified from *Saccharomyces cerevisiae* cell wall through alkali treatment, produced near identical effects as *C. albicans* β -glucan. However, untreated zymosan produced a distinct training effect from β -glucans at both the transcript and cytokine level. Training with zymosan diminished, rather than potentiated, induction of cytokines such as TNF and IL-6. Zymosan activated NF κ B and AP-1 transcription factors more strongly than β -glucans. The addition of the toll-like receptor (TLR) ligand Pam3CSK4 was sufficient to convert the training effect of β -glucans to a phenotype resembling zymosan. We conclude that differential activation of TLR signaling pathways determines the phenotype of innate immune training induced by Dectin-1 ligands.

There is growing recognition that cells of the innate immune system, such as monocytes and macrophages, retain memory of prior exposures. This innate immune “training” produces phenotypic shifts that alter macrophage responses to subsequent immune threats^{1,2}. Innate immune training carries therapeutic potential to enhance immune responses to heterologous pathogens^{3,4} or as a novel strategy for cancer immune therapy⁵. Innate immune training may also contribute to the pathogenesis of both hyper- and hypo-inflammatory disease states^{6,7}.

Unlike T- and B-cells of the adaptive immune system, which encode memory of prior exposures through genetic rearrangement, innate immune cells retain memory through non-genetic mechanisms such as metabolic reprogramming⁸ and epigenetic modifications⁹. Importantly, while the most widely used training ligands increase (or “potentiate”) inflammatory cytokine production, other training ligands have been shown to diminish inflammatory cytokine production^{10,11}. A key question in the field is what determines whether a given training ligand and the cell signaling pathways it activates will produce potentiated or diminished inflammatory responses.

One archetypal training ligand has been the fungal pathogen, *Candida albicans*, and the primary pathogen-associated molecular pattern (PAMP) found in its cell wall, 1,3- β -D-glucan^{12–14}. In vivo injection of β -glucan protects mice against subsequent infection with a broad range of heterologous pathogens³. β -glucan exposure in vivo produces trained macrophages that respond to secondary lipopolysaccharide (LPS) stimulation with increased production of inflammatory cytokines¹². This potentiation of cytokine production is also observed in human monocyte-derived macrophages trained in vitro with β -glucan¹⁵. The β -glucan training effect is dependent on the Dectin-1/Raf-1/mTOR signaling axis^{12,16} and is correlated with changes in chromatin accessibility and H3K27ac marks⁹ as well as a shift towards aerobic glycolysis⁸.

Notably, these insights were gained from studies that utilized a preparation of β -glucan that is not commercially available but has been generously shared by the Williams lab at East Tennessee State University (ETSU). This

¹Department of Medicine, Division of Infectious Diseases, David Geffen School of Medicine, University of California, Los Angeles, CA, USA. ²Molecular Biology Institute, University of California, Los Angeles, CA, USA. ³Department of Microbiology, Immunology, and Molecular Genetics, University of California, Los Angeles, CA, USA. ⁴Department of Surgery, Center of Excellence in Inflammation, Infectious Disease and Immunity, Quillen College of Medicine, East Tennessee State University, Johnson City, TN, USA. ✉email: quencheng@ucla.edu

highly purified (1 → 3,1 → 6)-β-glucan is isolated from *Candida albicans* SC5314 yeast cell walls and has been thoroughly characterized^{17,18}. However, commercially available “β-glucan” products are much more chemically and structurally diverse. Zymosan, one of the most widely used PAMPs in fungal pathogenesis studies, is a complex mixture of unpurified *Saccharomyces cerevisiae* cell wall. Although β-glucan is the most prevalent macromolecule in zymosan, these particles also contain mannoproteins, lipids, protein, chitin, and other macromolecules in variable proportions¹⁹ and therefore binds toll-like receptors (TLRs) in addition to Dectin-1^{20–22}. “Depleted zymosan” is a commercially available product in which zymosan is treated with hot alkali. This treatment depletes mannoproteins and chitin, resulting in a relatively pure β-glucan derived from *S. cerevisiae* that binds Dectin-1 with higher specificity²³. Whether zymosan and depleted zymosan produce similar innate immune training phenotypes to the archetypal β-glucan from ETSU is not known.

We show here that different Dectin-1 ligands can in fact produce distinct phenotypes of innate immune training. The commercially available β-glucan, depleted zymosan, has nearly identical effects to ETSU β-glucan. But untreated zymosan produces a distinct training regimen, exerting the opposite effect on key inflammatory cytokines. These differences arise from zymosan-specific activation of NFκB and AP-1 transcription factors and can be replicated by concurrent training with a TLR ligand plus β-glucan. Our study thus identifies important differences between fungal cell wall ligands and sheds light on underlying mechanisms that may determine the stimulus-specificity of innate immune training beyond these ligands.

Results

Training with zymosan and β-glucans induce different cytokine responses to LPS

To determine the specificity of different fungal cell wall ligands in trained immunity, we employed a well-established in vitro trained immunity model using primary human monocytes¹⁵. Monocytes were isolated from healthy human donors and differentiated to macrophages with MCSF, with or without training on Day 0 (Fig. 1A). On Day 7, we assessed response to secondary stimulation by measuring TNF production after stimulation with low-dose LPS (1 ng/mL). Consistent with the literature, TNF production was potentiated when macrophages were trained with *C. albicans* β-glucan (β-glu_{ETSU}) with a mean fold-change of 1.99 relative to Untrained ($p = 0.002$) (Fig. 1B). Training with depleted zymosan (β-glu_{DZ}) also potentiated TNF production, with mean fold-change of 1.97 ($p < 0.001$). Surprisingly, we found that training with untreated zymosan produced the opposite effect, diminishing TNF production with a mean fold-change of 0.34 ($p < 0.001$). This effect was consistent across a range of doses (Fig. S1), and was specific for particulate β-glucan. Soluble β-glucan, which does not activate Dectin-1 signaling²⁴, did not produce any immune training effect (Fig. S2).

To characterize training effects on a larger number of secreted proteins, we performed multiplexed bead-array cytokine measurements. Unsupervised hierarchical clustering revealed that a wide range of cytokines and chemokines behaved similarly to TNF, with diminished production in zymosan-trained macrophages and stable or potentiated production in depleted zymosan or ETSU β-glucan-trained macrophages (Fig. 1C). These included classic inflammatory cytokines TNF, IL-6, and IL-12P40; chemokines critical for phagocyte recruitment such as IP-10, MIP-1a, and MIP-1b; and growth factors such as GM-CSF and G-CSF.

Interestingly, this effect was not universal, and individual cytokines displayed nuanced effects. For instance, IL-1α was generally potentiated by all three training regimens. IL-10 was more strongly potentiated by ETSU β-glucan than depleted zymosan, while FGF-2 was only potentiated by depleted zymosan but not ETSU β-glucan.

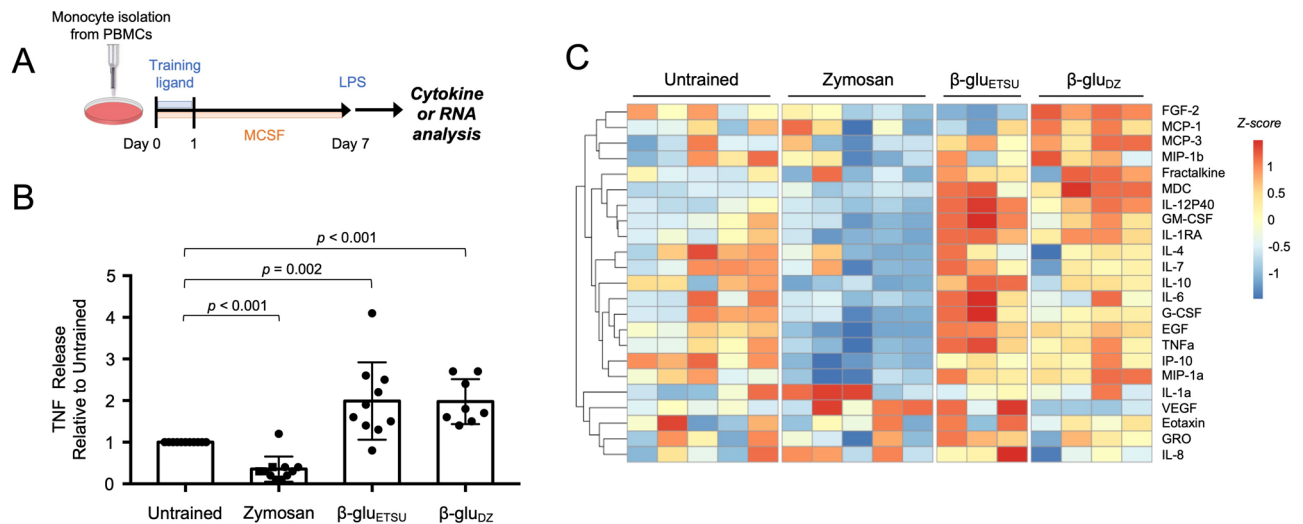


Figure 1. Training with zymosan and β-glucans induce different cytokine responses to LPS. (A) Experimental scheme. (B) TNF ELISA from supernatants of macrophages stimulated with LPS for 8 h, after training with the indicated ligands; p -values derived from two-tailed t -test; β-glu_{ETSU} = β-glucan from East Tennessee State University, β-glu_{DZ} = depleted zymosan. (C) Heat map of multiplexed cytokine bead array from supernatant of macrophages stimulated with LPS for 8 h, after training with the indicated ligands; replicate columns within a condition are from a different donors.

These data indicated that the effects of innate immune training are gene-specific, and that distinct regulatory strategies may exist for individual cytokines. Variability between replicates, such as was observed for IL-1 α , may also indicate that subtle differences in culture conditions may influence the training effect. Broadly speaking, however, we concluded that ETSU β -glucan and depleted zymosan produced similar training effects, in stark contrast to zymosan which diminished the production of most cytokines.

Training with zymosan and β -glucans induce different transcriptomic responses to LPS

Having established the differential training effects on secretion of cytokines, we wondered whether zymosan and β -glucans also exerted distinct effects on transcriptomic responses to LPS. We therefore trained monocytes and differentiated them to macrophages as before, then performed RNA-seq analysis. Samples were collected on Day 7 prior to secondary LPS stimulation (0 h), and at 1 and 3 h after LPS exposure. Experiments were performed in biological replicates with monocytes from different donors. We focused our analysis on 603 genes that were inducible by LPS in any training regimen, using a false discovery rate (FDR) cutoff of 0.05 and a \log_2 fold-change cutoff of 1.0 (Table S1). Using unsupervised k-means clustering, we identified five distinct patterns of gene expression (Fig. 2A). Cluster 1 genes had diminished LPS-responsiveness when trained with zymosan, but potentiated LPS-responsiveness when trained with either ETSU β -glucan or depleted zymosan. The differences in Cluster 1 gene expression between untrained, zymosan and β -glucan training was statistically significant ($p < 0.001$ for all comparisons), with median \log_2 (RPKM) differences of 0.769 for ETSU β -glucan versus zymosan and 0.915 for depleted zymosan versus zymosan (Fig. 2B). Cluster 1 included genes that encode cytokines potentiated by β -glucan training (Fig. 1C), such as *IL1RN* (IL1RA), *CSF2* (GM-CSF), *CSF3* (G-CSF), and *IL12B* (IL12p40). In contrast, Cluster 5 genes had the opposite pattern: potentiation when trained with zymosan and diminished responsiveness when trained with a β -glucan. These differences were also statistically significant, with median \log_2 (RPKM) differences of -0.892 ($p < 10^{-16}$) and -0.887 ($p < 10^{-16}$) for ETSU β -glucan and depleted zymosan, respectively (Fig. 2B). Cluster 2, 3, and 4 genes had diminished LPS-responsiveness in all three training regimens; these three clusters were distinguished from one another based on kinetics of gene induction.

Next, we quantified the differential effects of training. For each trained condition, we defined the training effect by calculating \log_2 (fold-change) of trained versus untrained at each timepoint. We found that training with ETSU β -glucan and depleted zymosan produced highly correlated effects; for example, at the 3-h timepoint, the correlation coefficient was 0.941 (Fig. 2C). In contrast, the correlation coefficient between the effects of untreated zymosan and depleted zymosan was only 0.518 (Fig. 2C). Although zymosan and depleted zymosan exerted the same effect on some genes, such as *CXCL11*, *IFNB*, and *DDIT4*, they had disparate effects on other genes such as *SERPINB2*, *IL12B*, and *IL23*. Visualizing the correlation matrix for pairwise comparisons between all training regimens further strengthened the observation that ETSU β -glucan and depleted zymosan exert similar training effects while zymosan produces a distinct effect (Fig. 2D). These analyses demonstrated that training with zymosan versus β -glucans produces distinct transcriptomic responses to LPS.

We next sought to stringently identify genes that were differentially expressed after training. Among the 603 LPS-inducible genes, we identified 72 genes that were potentiated and 277 genes that were diminished by any training regimen, using a p -value cutoff of < 0.05 and a \log_2 fold-change cutoff (trained vs. untrained) of > 0.5 . Of the diminished genes, 100 out of 277 (36.1%) were shared between untreated zymosan and the β -glucans (Fig. 2E), consistent with the qualitative effect seen in Clusters 2, 3, and 4 of the heatmap (Fig. 2A). In contrast, only 7 out of 72 potentiated genes (9.7%) were shared between untreated zymosan and the β -glucans, further evidence of their divergent training effects. The set of potentiated genes included key immune regulators such as *PTGIR* and *WNT5A* (potentiated by zymosan), *IL12B* (potentiated by β -glucans), and *IL1A* (potentiated by both at the 3h timepoint) (Fig. 2F,G). Given the small number of genes, no statistically significant enrichment of gene ontology terms was detected (using 603 LPS-inducible genes as the reference gene set).

Zymosan and β -glucans activate distinct signaling networks

Having established differences between zymosan and β -glucans at both the secreted cytokine and transcriptomic levels, we next examined which signaling pathways and transcription factors were activated by these ligands. All three ligands are known to engage Dectin-1²⁵, but in murine myeloid cells and human cell lines untreated zymosan also engages TLRs, specifically TLR2^{21,22}. Whether these ligand-receptor interactions hold true in primary human monocytes is uncertain. Furthermore, what nuclear transcription factors are activated downstream of these ligands in this system is not clear. To address these questions, we performed immunoblot on nuclear extracts of monocytes stimulated with zymosan or β -glucan. As ETSU β -glucan and depleted zymosan were shown to produce nearly identical training effects, we considered these two ligands functionally equivalent and focused our signaling studies on ETSU β -glucan given its prominence in the literature.

We found that zymosan rapidly and robustly induced nuclear localization of NF κ B p65 and phosphorylated AP-1 family member cJUN (Fig. 3A). Surprisingly, zymosan also induced nuclear localization of phosphorylated IRF3. This was unexpected given zymosan's reported interaction with Dectin-1 and TLR2, neither of which would be expected to activate the TRIF-IRF axis. Zymosan also activated STAT1, likely due to secondary signaling from IRF3-induced type I interferon (IFN)²⁶. In contrast to zymosan, ETSU β -glucan only weakly activated NF κ B p65 and cJUN at 1 h and did not detectably activate IRF3 or STAT1 (Fig. 3A). Quantification of immunoblots showed that β -glucan-induced nuclear NF κ B p65 abundance was consistently less than zymosan-induced p65 at 1 h, with a mean reduction of 48% over four replicates, $p = 0.020$ (Fig. 3B). β -glucan-induced nuclear accumulation of phosphorylated c-JUN was also less than zymosan-induced c-JUN at 1 h, with a mean reduction of 74% over four replicates, $p < 0.001$ (Fig. 3B). Taken together, these data indicate that zymosan activates signaling pathways that β -glucans do not, likely through engagement of additional TLRs.

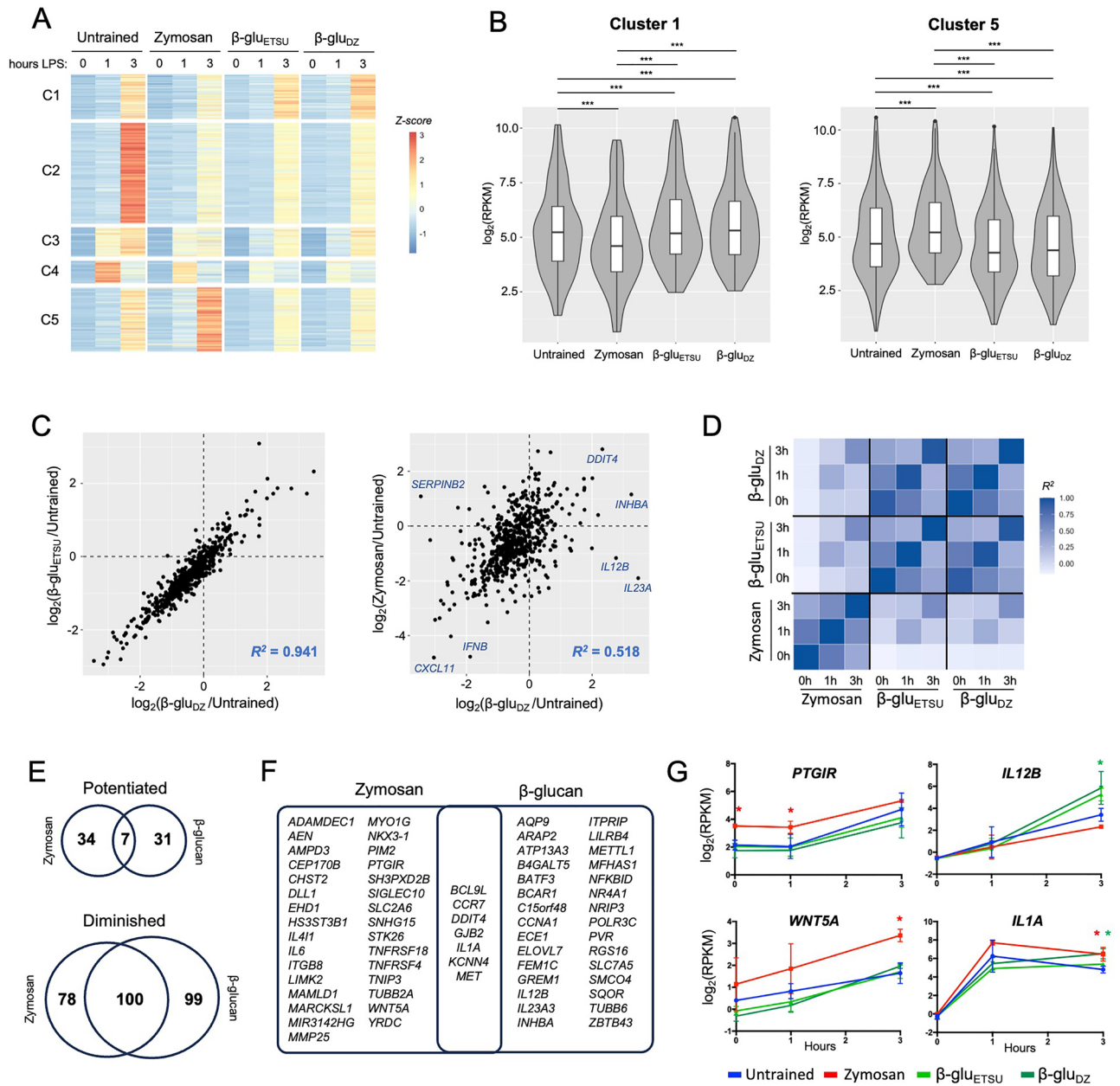


Figure 2. Training with zymosan and β -glucans induce different transcriptomic responses to LPS. **(A)** Heat map of 603 genes induced by LPS over a 3-h time course in macrophages trained with the indicated ligands; average of two replicates; k-means clustering showing five distinct clusters. **(B)** Box and violin plots of RPKM at 3 h for genes in Cluster 1 and Cluster 5; *** $p < 0.001$ by paired t-test. **(C)** Scatterplots comparing log fold-change of trained versus untrained RPKM at 3-h LPS timepoint; training effect of two types of β -glu are strongly correlated with each other (left), but weakly correlated with zymosan effects (right). **(D)** Heat map of correlation coefficients between conditions using the same analytical approach as (C). **(E)** Venn diagrams of the number of genes showing potentiated or diminished LPS response after training with Zymosan or either β -glu, using statistical threshold of $p < 0.05$ and log fold-change > 0.5 . **(F)** Venn diagram of genes with potentiated LPS response after training. **(G)** Expression of representative genes potentiated by Zymosan (*PTGIR*, *WNT5A*), β -glu (*IL12B*), or both (*IL1A*); error bars = standard deviation, * = $p < 0.05$ in condition indicated by color.

We hypothesized that differences in composition of these ligands may lead to differential activation of cell signaling pathways to produce distinct training effects. We first examined whether our ligands contained trace amounts of LPS. Using a qualitative Limulus amoebocyte lysate (LAL) assay, we found that LAL reacted with zymosan (1 $\mu\text{g/ml}$) but not depleted zymosan (10 $\mu\text{g/ml}$) or ETSU β -glu (10 $\mu\text{g/ml}$). As β -glucans can cause false positives in LAL assays, we confirmed this result using HEK-Blue TLR4 cells in which 293T cells express TLR4 and secreted embryonic alkaline phosphatase (SEAP) under an NF κ B-inducible promoter. We found that 1 $\mu\text{g/ml}$ zymosan induced expression of SEAP comparable to 1 ng/ml LPS (Fig. 3C). Neither of the pure β -glucans

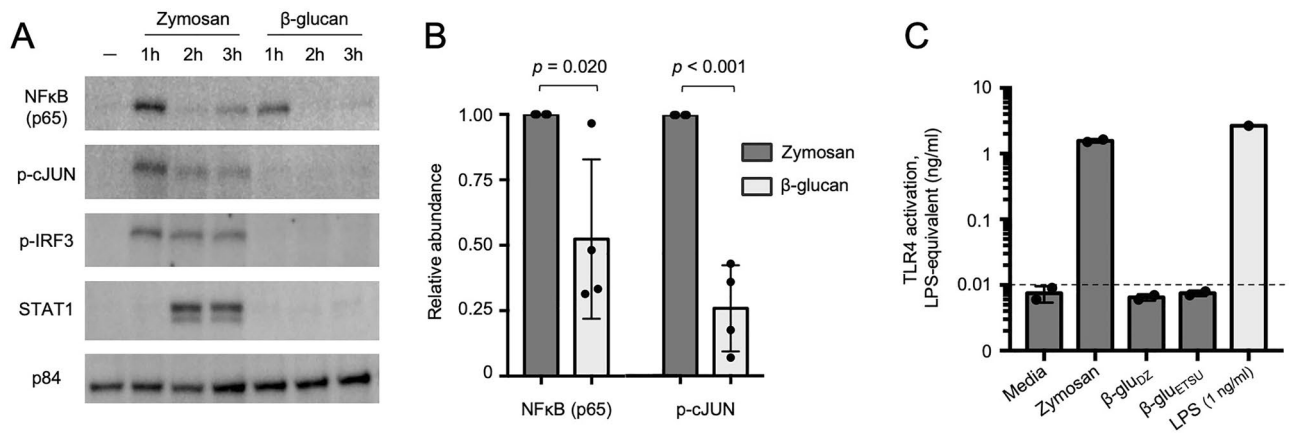


Figure 3. Zymosan and β -glucans activate distinct signaling networks. (A) Immunoblot of nuclear extracts of monocytes stimulated with zymosan or ETSU β -glucan over a 3-h timecourse. Representative image from four replicates. (B) Quantification of nuclear NFkB (p65) and phospho-cJUN at 1 h after stimulation with indicated ligands, normalized to p84, aggregate of four replicates. (C) TLR4 activity measured by NFkB-induced SEAP activity in HEK-Blue TLR4 cells, quantified using LPS standard curve; dashed line represents limit of quantitation; zymosan 1 μ g/ml, β -glu_{DZ} and β -glu_{ETSU} 10 μ g/ml.

nor media alone induced SEAP expression. We concluded that zymosan, but not depleted zymosan or ETSU β -glucan, likely contained biologically active amounts of endotoxin, thus explaining zymosan's ability to induce IRF3 and STAT1 through TLR4. As LPS has been a well-established inducer of tolerance²⁷, these results provide a plausible explanation for the observed training effects of zymosan.

We next performed proton nuclear magnetic resonance (NMR) to further evaluate the composition of each ligand. Consistent with the possible presence of endotoxin, we found that untreated zymosan contained more lipid and protein, reflected in greater NMR signal between 0.5 and 2.8 ppm²⁸ (Fig. S2A). These NMR peaks were diminished in depleted zymosan, while the β -glucan from ETSU was nearly devoid of protein and lipid components. Depleted zymosan was composed of 85% carbohydrate, of which 80% was glucan and 11% glycogen. Its (1,6)- β -D-glucan side chains had an average length of 4.2 repeats with an average branching frequency of 12.4 repeats. ETSU β -glucan was nearly 100% carbohydrate with no detectable glycogen. Its glucan had longer (1,6)- β -D-glucan side chains with an average of 12.8 repeats and similar average branching frequency of 14.6 repeats (Fig. S2B). In contrast, untreated zymosan was too impure to allow calculation of the carbohydrate structure. This structural analysis supported our observations that depleted zymosan and ETSU β -glucan had only subtle differences, while zymosan differed significantly.

Concurrent exposure to TLR ligand, but not IFN β , reverses β -glucan training

Our biochemical analysis indicated that due to the differences in its composition, zymosan engages TLRs, activating both MyD88 and TRIF pathways, in ways that β -glucans do not. To test the hypothesis that concurrent TLR stimulation produces distinct immune training phenotypes, we trained with mixtures of ligands using the same protocol as before, followed by secondary LPS stimulation and cytokine measurement. Pam3CSK4 is a TLR2-specific agonist that activates NFkB and AP-1 pathways without activating the IRF3-STAT1 axis (Fig. S4), while IFN β directly activates STAT1²⁶. We found that concurrent exposure to Pam3CSK4 reduced the β -glucan-mediated potentiation of TNF release by 51% ($p = 0.048$), while the addition of IFN β had no effect (Fig. 4A). These effects were largely conserved across a panel of cytokines measured by multiplexed bead array. Addition of Pam3CSK4 generally inhibited the training effects of β -glucan, producing a phenotype similar to zymosan, while addition of IFN β preserved or in some cases enhanced the training effect of β -glucan (Fig. 4B). Interestingly, for a small number of cytokines, the combination of β -glucan and Pam3CSK4 did not recapitulate the effect of zymosan. One of these exceptions was IL-1 α , where zymosan potentiated cytokine release while β -glucan diminished it, and addition of Pam3CSK4 did not alter the β -glucan effect. For most cytokines, however, we concluded that concurrent activation of MyD88 pathways through TLR2 stimulation was sufficient to reverse the effects of β -glucan training.

Discussion

Innate immune training using prototypical stimuli such as β -glucan has potent effects, yet the determinants of stimulus-specificity in trained immunity remain unclear. β -glucans train innate immune cells through the Dectin-1 receptor^{12,16}, but there are many different Dectin-1 ligands, both commercially available preparations as well as the widely published β -glucan from ETSU. These ligands have important differences in their preparation and structure that may lead to differences in innate immune training. We found that *C. albicans*-derived β -glucan from ETSU and *S. cerevisiae*-derived β -glucan (depleted zymosan) are nearly identical in their training effect. But unpurified zymosan induces a training regimen that is distinct from β -glucans, and in the case of many cytokines exerts the opposite effect. Zymosan triggers TLR activation and robustly induces NFkB activity, likely

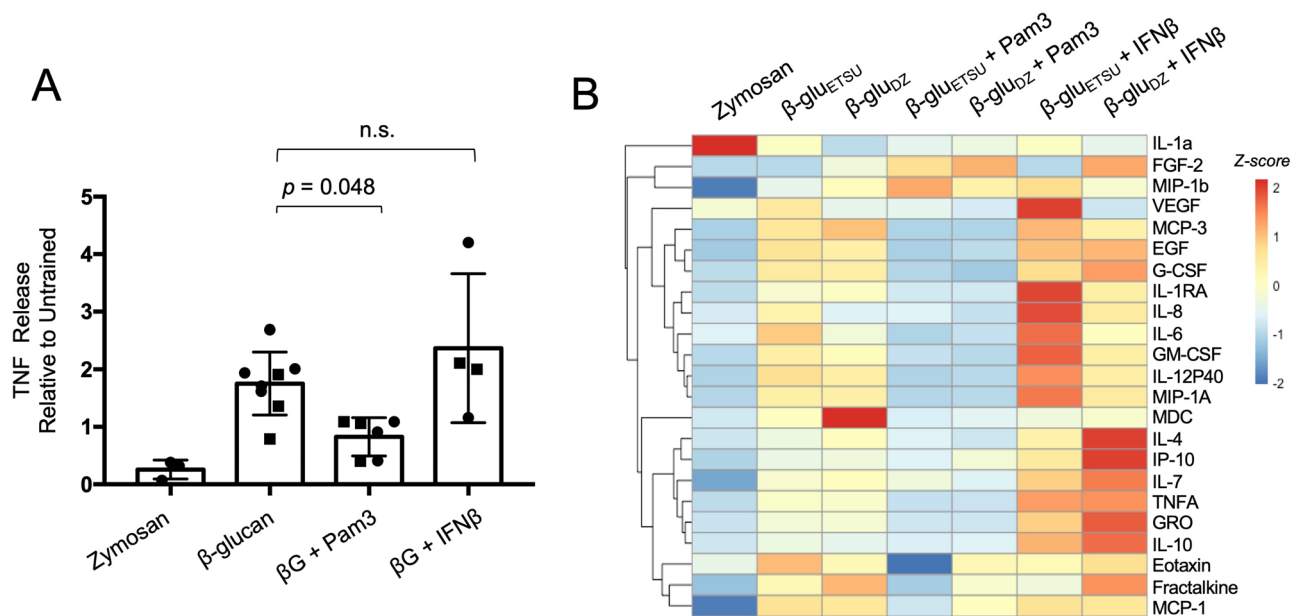


Figure 4. Concurrent exposure to TLR ligand, but not IFN β , reverses β -glucan training. **(A)** TNF ELISA from supernatants of macrophages stimulated with LPS for 8 h, after training with the indicated ligands; *p*-values derived from two-tailed t-test, n.s. = not significant. Squares = ETSU, circles = depleted zymosan. **(B)** Heat map of multiplexed cytokine bead array from supernatant of macrophages stimulated with LPS for 8 h, after training with the indicated ligands.

through the concurrent presence of endotoxin. This produces a tolerance effect that overrides the potentiation effect of training with β -glucans.

Our study demonstrates that not all Dectin-1 ligands are equal with respect to innate immune training. It is particularly notable that one of the most widely used Dectin-1 agonists in the fungal pathogenesis literature (zymosan) produces dramatically different effects from the most widely published Dectin-1 agonist in the trained immunity literature (β -glucan from ETSU). Investigators in both fields would be well-served to carefully consider their choice of Dectin-1 ligand. Our results also underscore the importance of ligand purity and composition. We found that zymosan reacts with LAL and triggers NF κ B activity in HEK-Blue TLR4 cells. It is possible that the HEK-Blue TLR4 assay was positive due to other signaling pathways activating NF κ B, such as TLR3, TLR5, or TNFR, which are endogenously expressed on HEK-293T cells. However, the positive LAL assay supports the interpretation that the presence of endotoxin is the likely explanation for zymosan's training effect. While it is unclear if zymosan from other manufacturers behave similarly, it is worth noting that the zymosan product we used has been widely employed in the literature.

A key insight from our study is that activation of TLR signaling is sufficient to override the training effect of β -glucans. At the signaling level, we found that zymosan strongly activates MyD88-dependent NF κ B and AP-1 transcription factors, as well as the TRIF-dependent IRF-STAT axis. In contrast, β -glucans only weakly activate NF κ B and AP-1 and do not activate IRF-STAT pathways. Remarkably, addition of the TLR2 ligand Pam3CSK4 largely reversed the training effect of β -glucans, whereas addition of IFN β did not. Others have shown that training with Pam3CSK4 and other TLR ligands diminishes TNF production in both murine and human macrophages^{11,29}. Our study extends these findings to demonstrate that when monocytes are concurrently trained with Pam3CSK4 and β -glucan, the TLR-induced activation of MyD88-dependent NF κ B and AP-1 pathways dominates sufficiently to inhibit the training effect of β -glucan.

Our observation that TLR activation opposes the training effect of β -glucans carries significant implications for the broader application of trained immunity. It is not known, for instance, how simultaneous exposure to different training ligands in vivo may alter response to subsequent infections. This is particularly relevant when considering that pathogens may train the immune system in one direction while simultaneously causing the release of cytokines and DAMPs that may produce opposing training effects. Thus, additional studies will be needed to define the mechanisms by which TLR activation opposes β -glucan-induced training. As trained immunity is thought to be encoded through modifications to the epigenome, one possibility is that TLR activation enforces an opposing epigenomic program. Stimulus-specific epigenomic reprogramming can occur even when similar transcription factors are activated due to differences in distinct patterns of temporal activity³⁰.

One of the strengths of our study is the characterization of innate immune training across a wide array of secreted cytokines and the entire transcriptome. Much of the literature in this field has focused on archetypal inflammatory cytokines such as TNF, but relatively few studies have examined effects genome-wide. By utilizing systems-level analyses we show that innate immune training is both stimulus-specific and gene-specific. That is, different stimuli produce different training effects, but each gene is uniquely regulated. For example, zymosan and β -glucans induce opposing training effects on IL-6, but they have the same effect on IL-1 α . It is likely that

studies which focus on one or two inflammatory cytokines underestimate the complexity of training effects. These studies have led to the proposal that “trained immunity” can be defined by a potentiation of inflammatory cytokines like TNF, while “tolerance” is defined by a reduction in the same cytokines³¹. We suggest that rigid definitions of “training” and “tolerance” obscure subtle differences in immune training phenotypes, akin to the oversimplified paradigm of “M1” and “M2” macrophages³².

Interestingly, whole *C. albicans* yeasts, which activate both Dectin-1 and TLR2³³, potentiate expression of TNF and IL6¹². In fact, mannans sensed by TLR2 are required for maximal potentiation of TNF by *C. albicans* in vivo¹⁶. While this seems at odds with our observations regarding TLR co-stimulation, three mechanisms could explain the apparent discrepancy. First, there are likely substantial differences in the relative availability of TLR2 binding sites between fragmented *S. cerevisiae*-derived cell walls (zymosan) and intact *C. albicans* yeasts³³. Secondly, it is possible that complex regulatory mechanisms exist in vivo that dampen the TLR-mediated effects³⁴; this would also explain why others have observed that zymosan injection in vivo slightly increases intracellular TNF in splenic macrophages³⁵. Thirdly, *C. albicans* interacts with multiple other host receptors in vivo, such as NLRP3, CR3, and mannose receptors, all of which have the potential to influence trained immunity³⁶.

Our understanding of the mechanisms underlying innate immune training remains incomplete, but this study advances the field by showing that widely utilized Dectin-1 ligands produce distinct phenotypes of immune training across a broad range of cytokines and genes. The fact that TLR activation reverses the training effect of β -glucan may provide important clues to further unravel the mechanisms of innate immune training.

Methods

Reagents

C. albicans β -glucan was generously provided by Dr. David Williams at ETSU. Sterility of the glucan was confirmed as previously described²⁸. Zymosan and depleted zymosan were purchased from InvivoGen (tlrl-zyn, tlrl-zyd). Endotoxin testing and characterization by NMR are described below.

Tissue culture

Peripheral blood mononuclear cells were obtained from healthy donors through the UCLA-CFAR Virology Core. Monocytes were isolated by negative bead selection using a Pan-Monocyte Isolation Kit (Miltenyi Biotec 130-096-537) with LS columns (Miltenyi Biotec 130-042-401) and grown in 24-well tissue culture plates (Corning) at a seeding density of 250,000 to 500,000 cells per well in 1 mL of complete medium consisting of RPMI 1640 broth containing 10% fetal bovine serum (Gibco), 100 IU/ml penicillin, 100 μ g/ml streptomycin, 2 mM L-glutamine, and 10 ng/ml recombinant human M-CSF (R&D Systems 216-MC-100) at 37 °C for 7 days.

In vitro immune training

Monocytes were rested in complete medium for 30–60 min after purification, then trained with the following ligands for 24 h in a final volume of 1 mL per well of a 24-well plate: zymosan (1 μ g/mL), ETSU β -glucan (10 μ g/mL), depleted zymosan (10 μ g/mL), Pam3CSK4 (100 ng/mL, Invivogen tlrl-pms), or IFN- β (10 U/mL, PBL Assay Science 11415-1). After 24 h of training, the medium was aspirated, cells were washed with warm HBSS, and fresh complete medium was added. On Day 4, medium was aspirated and fresh medium was added. On Day 7, the cells were stimulated with LPS (1 ng/mL, Millipore Sigma L6529) and analyzed for cytokine release or gene expression.

Cytokine release assays

For cytokine release assays, monocytes were plated at different concentrations to account for the variable effects of trained immunity on cell proliferation rates¹⁵. On Day 7, wells with similar cell densities by microscopy were chosen for comparisons between training regimens. Medium was removed, centrifuged to remove non-adherent cells, and snap-frozen for cytokine measurement. TNF- α concentration was determined by sandwich ELISA (R&D Systems DY210-05) per manufacture protocol. Multiplex bead-based measurements of cytokines (Luminex, Thermo Fisher) were performed by the UCLA Immune Assessment Core using a panel of 38 analytes.

Luminex analysis

Data were quantified using standard curves provided by the manufacturer. Analytes expressed at levels below the lowest standard were excluded from downstream analysis. To account for variability in cell density and absolute cytokine concentrations between biological replicates, each replicate was Z-scored across samples.

RNA extraction and RT-qPCR

Cells were lysed using Qiagen RNeasy Micro Kit (Qiagen 74004), and RNA was extracted according to manufacturer’s protocol. Reverse transcription was carried out using LunaScript RT (New England Biolabs E3010) per manufacturer’s protocol. Quantitative PCR was performed with Luna® Universal qPCR Master Mix (New England Biolabs M3003). CT values for *IL12B* were normalized against housekeeping gene *HPRT*. The following primer sequences were used: *IL12B* – GCCCAGAGCAAGATGTGTCA, CACCATTCTCCAGGGGCAT; and *HPRT* – AGGACTGAACGTCTTGCTCG, ATCCAACACTTCGTGGGGTC.

RNA-sequencing

RNA-seq libraries were prepared using KAPA stranded mRNA-seq library kit per manufacturer’s instructions and single-end sequenced at read length 50 bp on an Illumina HiSeq 2500 to a depth of 15–30 million reads per library. The low quality 3’ends of reads were trimmed (cutoff q = 30), and remaining adapter sequences were

removed using cutadapt³⁷. Processed reads were aligned to hg38 genome using STAR³⁸, and count tables were generated by the featureCount function in deepTools³⁹. Counts were normalized using the TMM-normalization method and RPKM values were generated using edgeR⁴⁰. Genes below an expression threshold of 4 CPM in all samples were excluded from downstream analysis. LPS-inducible genes were identified by $FDR < 0.05$ and $\log_2(\text{fold-change}) > 2$ compared to unstimulated. Potentiated or diminished LPS-responses were identified by refitting the linear model to the 603 LPS-inducible genes and imposing thresholds of $p\text{-value} < 0.05$ and $\log_2(\text{fold-change}) > 0.5$ comparing trained versus untrained gene expression. For \log_2 transformations and fold-change calculations a pseudocount of 0.63 RPKM was added. The data were visualized using pheatmap and ggplot2 packages^{41,42}.

Nuclear magnetic resonance

Zymosan, depleted zymosan, and *C. albicans* β -glucan were dissolved in DMSO- d_6 at 10 mg/ml and 20 μ L TFA-d was added. NMR data was collected at 60 °C on a Bruker AvanceCore 400 spectrometer with 65,536 data points, 2 dummy scans, 128 scans, 1-s pulse delay and 20.5 ppm sweep width centered at 6.175 ppm. Identification of carbohydrate, protein, and lipid composition and carbohydrate structure was performed as previously described²⁸.

Immunoblots

Monocytes were isolated from PBMCs as above and cultured for 24 h in M-CSF-containing medium to allow for adherence. Cells were then stimulated with the same concentrations of ligands as in the trained immunity assays. At the designated timepoints, cells were rinsed with cold PBS and detached using a cell scraper. The cytoplasmic membrane was lysed in hypotonic buffer (10 mM 7.9 pH HEPES, 10 mM KCl, 0.1 mM EGTA, 0.1 mM EDTA) containing 1% NP-40. Nuclei were pelleted by centrifugation, and nuclear proteins were extracted in hypertonic solution (20 mM 7.9 pH HEPES, 420 mM NaCl, 1.5 mM MgCl₂, 0.2 mM EDTA, 25% Glycerol) with protease and phosphatase inhibitors.

Protein concentrations were measured using Bradford Protein Assay (BioRad) and normalized in nuclear lysis buffer. 2 × Laemmli Buffer (BioRad) containing 5% beta-mercaptoethanol was added, and samples were heated at 95 °C for 10–20 min, separated by SDS-PAGE, and transferred to nitro-cellulose membranes. The following antibodies were used for immunoblotting: p-cJUN (Rabbit IgG, 1:2000, Cell Signaling Technology 9164), pIRF-3 (Rabbit IgG, 1:1000, Cell Signaling Technology 4947), p65(RelA) (Rabbit IgG, 1:1000, Santa Cruz 372), p-STAT1 (Rabbit IgG, 1:1000, Cell Signaling Technology 9167), and p84 (Rabbit IgG, 1:10,000, 5E10), and anti-rabbit IgG (Goat IgG-HRP, 1:5000, Cell Signaling Technology 7074). Immunoblots were developed using chemiluminescent substrate (Supersignal West Pico Plus, Thermo Fisher) and visualized using a ChemiDoc MP imaging system (Bio-Rad, Hercules, CA). Following imaging, western blots were stripped for re-probing using a stripping buffer (ThermoFisher Scientific).

Endotoxin testing

Limulus amoebocyte lysate (LAL) assay was performed using Thermo Fisher Scientific Pierce Rapid Gel Clot Endotoxin Assay (ThermoFisher Scientific A43879) according to manufacturer's instructions. TLR4 bioactivity was assayed with Human TLR4 Reporter HEK293 Cells (Invivogen hkb-hltr4). TLR4-expressing HEK293T reporter cells were plated at 50,000 cells per well in 96 well plates in DMEM with 10% fetal bovine serum (Gibco), 100 IU/ml penicillin, 100 μ g/ml streptomycin, and 2 mM L-glutamine. Zymosan (1 μ g/ml), depleted zymosan (10 μ g/ml), and ETSU β -glucan (10 μ g/ml) were added to a final volume of 150 μ L. A standard curve was generated with serial tenfold dilutions of LPS. Negative controls were performed with media alone and stimulation of parent HEK293 Null2 cells (Invivogen hkb-null2) plated in an identical manner to TLR4-reporter cells. After 20 h incubation at 37C, cell culture media were collected, centrifuged to clear cell debris, and developed with Quanti-Blue reagent (Invivogen rep-qbs) according to manufacturer's instructions. After 20 min incubation at 37C, absorbance at 630 nm was measured using a standard 96-well plate reader.

Data availability

Raw data and count tables for this study are available at Gene Expression Omnibus (GEO) under accession number GSE242947. Code used in data analysis can be provided upon request by contacting the corresponding author.

Received: 27 October 2023; Accepted: 8 January 2024

Published online: 17 January 2024

References

1. Netea, M. G. *et al.* Defining trained immunity and its role in health and disease. *Nat. Rev. Immunol.* **20**, 375–388. <https://doi.org/10.1038/s41577-020-0285-6> (2020).
2. Netea, M. G. *et al.* Trained immunity: A program of innate immune memory in health and disease. *Science* **352**, aaf1098. <https://doi.org/10.1126/science.aaf1098> (2016).
3. Ciarlo, E. *et al.* Trained immunity confers broad-spectrum protection against bacterial infections. *J. Infect. Dis.* **222**, 1869–1881. <https://doi.org/10.1093/infdis/jiz692> (2020).
4. Giamarellos-Bourboulis, E. J. *et al.* Activate: Randomized clinical trial of BCG vaccination against infection in the elderly. *Cell* **183**, 315–323. <https://doi.org/10.1016/j.cell.2020.08.051> (2020).
5. Kalafati, L. *et al.* Innate immune training of granulopoiesis promotes anti-tumor activity. *Cell* **183**, 771–785. <https://doi.org/10.1016/j.cell.2020.09.058> (2020).
6. Geng, S. *et al.* The persistence of low-grade inflammatory monocytes contributes to aggravated atherosclerosis. *Nat. Commun.* **7**, 13436. <https://doi.org/10.1038/ncomms13436> (2016).
7. Sun, K. & Metzger, D. W. Inhibition of pulmonary antibacterial defense by interferon-gamma during recovery from influenza infection. *Nat. Med.* **14**, 558–564. <https://doi.org/10.1038/nm1765> (2008).

8. Cheng, S.-C. *et al.* mTOR/HIF1 α -mediated aerobic glycolysis as metabolic basis for trained immunity. *Science* **345**, 1250684. <https://doi.org/10.1126/science.1250684> (2014).
9. Saeed, S. *et al.* Epigenetic programming of monocyte-to-macrophage differentiation and trained innate immunity. *Science* **345**, 1251086. <https://doi.org/10.1126/science.1251086> (2014).
10. Finlay, C. M. *et al.* Helminth products protect against autoimmunity via innate type 2 cytokines IL-5 and IL-33, which promote eosinophilia. *J. Immunol. Baltim Md.* **1950**(196), 703–714. <https://doi.org/10.4049/jimmunol.1501820> (2016).
11. Ifrim, D. C. *et al.* Trained immunity or tolerance: Opposing functional programs induced in human monocytes after engagement of various pattern recognition receptors. *Clin. Vaccine Immunol. CVI* **21**, 534–545. <https://doi.org/10.1128/CVI.00688-13> (2014).
12. Quintin, J. *et al.* *Candida albicans* infection affords protection against reinfection via functional reprogramming of monocytes. *Cell Host Microbe* **12**, 223–232. <https://doi.org/10.1016/j.chom.2012.06.006> (2012).
13. Brown, G. D. *et al.* Dectin-1 is a major beta-glucan receptor on macrophages. *J. Exp. Med.* **196**, 407–412. <https://doi.org/10.1084/jem.20020470> (2002).
14. Goodridge, H. S., Wolf, A. J. & Underhill, D. M. Beta-glucan recognition by the innate immune system. *Immunol. Rev.* **230**, 38–50. <https://doi.org/10.1111/j.1600-065X.2009.00793.x> (2009).
15. Domínguez-Andrés, J. *et al.* In vitro induction of trained immunity in adherent human monocytes. *STAR Protoc.* **2**, 100365. <https://doi.org/10.1016/j.xpro.2021.100365> (2021).
16. Ifrim, D. C. *et al.* *Candida albicans* primes TLR cytokine responses through a dectin-1/Raf-1-mediated pathway. *J. Immunol.* **190**, 4129–4135. <https://doi.org/10.4049/jimmunol.1202611> (2013).
17. Lowman, D. W., Ferguson, D. A. & Williams, D. L. Structural characterization of (1 \rightarrow 3)- β -d-glucans isolated from blastospore and hyphal forms of *Candida albicans*. *Carbohydr. Res.* **338**, 1491–1496. [https://doi.org/10.1016/S0008-6215\(03\)00169-1](https://doi.org/10.1016/S0008-6215(03)00169-1) (2003).
18. Lowman, D. W. *et al.* Novel structural features in *Candida albicans* hyphal glucan provide a basis for differential innate immune recognition of hyphae versus yeast. *J. Biol. Chem.* **289**, 3432–3443. <https://doi.org/10.1074/jbc.M113.529131> (2014).
19. Ohno, N., Miura, T., Miura, N. N., Adachi, Y. & Yadomae, T. Structure and biological activities of hypochlorite oxidized zymosan. *Carbohydr. Polym.* **44**, 339–349. [https://doi.org/10.1016/S0144-8617\(00\)00250-2](https://doi.org/10.1016/S0144-8617(00)00250-2) (2001).
20. Underhill, D. M. *et al.* The Toll-like receptor 2 is recruited to macrophage phagosomes and discriminates between pathogens. *Nature* **401**, 811–815. <https://doi.org/10.1038/44605> (1999).
21. Gantner, B. N., Simmons, R. M., Canavera, S. J., Akira, S. & Underhill, D. M. Collaborative induction of inflammatory responses by dectin-1 and toll-like receptor 2. *J. Exp. Med.* **197**, 1107–1117. <https://doi.org/10.1084/jem.20021787> (2003).
22. Sato, M. *et al.* Direct binding of toll-like receptor 2 to zymosan, and zymosan-induced NF- κ B activation and TNF- α secretion are down-regulated by lung collectin surfactant protein A. *J. Immunol.* **171**, 417–425. <https://doi.org/10.4049/jimmunol.171.1.417> (2003).
23. Ikeda, Y. *et al.* Dissociation of toll-like receptor 2-mediated innate immune response to zymosan by organic solvent-treatment without loss of dectin-1 reactivity. *Biol. Pharm. Bull.* **31**, 13–18. <https://doi.org/10.1248/bpb.31.13> (2008).
24. Goodridge, H. S. *et al.* Activation of the innate immune receptor Dectin-1 upon formation of a 'phagocytic synapse'. *Nature* **472**, 471–475. <https://doi.org/10.1038/nature10071> (2011).
25. Mata-Martínez, P., Bergón-Gutiérrez, M. & del Fresno, C. Dectin-1 signaling update: New perspectives for trained immunity. *Front. Immunol.* **13**, 365 (2022).
26. Luecke, S., Sheu, K. M. & Hoffmann, A. Stimulus-specific responses in innate immunity: Multilayered regulatory circuits. *Immunity* **54**, 1915–1932. <https://doi.org/10.1016/j.immuni.2021.08.018> (2021).
27. Foster, S. L., Hargreaves, D. C. & Medzhitov, R. Gene-specific control of inflammation by TLR-induced chromatin modifications. *Nature* **447**, 972–978. <https://doi.org/10.1038/nature05836> (2007).
28. Kruppa, M. D. *et al.* Isolation, physicochemical characterization, labeling, and biological evaluation of mannans and glucans. *Methods Mol. Biol. Clifton NJ* **2542**, 323–360. https://doi.org/10.1007/978-1-0716-2549-1_24 (2022).
29. Divangahi, M. *et al.* Trained immunity, tolerance, priming and differentiation: Distinct immunological processes. *Nat. Immunol.* **22**, 2–6. <https://doi.org/10.1038/s41590-020-00845-6> (2021).
30. Murray, P. J. *et al.* Macrophage activation and polarization: Nomenclature and experimental guidelines. *Immunity* **41**, 14–20. <https://doi.org/10.1016/j.immuni.2014.06.008> (2014).
31. Bono, C. *et al.* Dectin-1 stimulation of hematopoietic stem and progenitor cells occurs in vivo and promotes differentiation toward trained macrophages via an indirect cell-autonomous mechanism. *mBio* **11**, e00781. <https://doi.org/10.1128/mBio.00781-20> (2020).
32. Cheng, Q. J. *et al.* NF- κ B dynamics determine the stimulus-specificity of epigenomic reprogramming in macrophages. *Science* **372**, 1349–1353. <https://doi.org/10.1126/science.abc0269> (2021).
33. Netea, M. G. *et al.* The role of toll-like receptor (TLR) 2 and TLR4 in the host defense against disseminated candidiasis. *J. Infect. Dis.* **185**, 1483–1489. <https://doi.org/10.1086/340511> (2002).
34. Pradhan, A. *et al.* Non-canonical signalling mediates changes in fungal cell wall PAMPs that drive immune evasion. *Nat. Commun.* **10**, 5315. <https://doi.org/10.1038/s41467-019-13298-9> (2019).
35. Park, H. J. *et al.* In vivo zymosan treatment induces IL15-secreting macrophages and KLRG1-expressing NK cells in mice. *Molecules* **28**, 5779. <https://doi.org/10.3390/molecules28155779> (2023).
36. Zheng, N.-X., Wang, Y., Hu, D.-D., Yan, L. & Jiang, Y.-Y. The role of pattern recognition receptors in the innate recognition of *Candida albicans*. *Virulence* **6**, 347–361. <https://doi.org/10.1080/21505594.2015.1014270> (2015).
37. Martin, M. Cutadapt removes adapter sequences from high-throughput sequencing reads. *EMBnet J.* **17**, 10. <https://doi.org/10.14806/ej.17.1.200> (2011).
38. Dobin, A. *et al.* STAR: Ultrafast universal RNA-seq aligner. *Bioinformatics* **29**, 15–21. <https://doi.org/10.1093/bioinformatics/bts635> (2013).
39. Liao, Y., Smyth, G. K. & Shi, W. featureCounts: An efficient general purpose program for assigning sequence reads to genomic features. *Bioinforma Oxford Engl.* **30**, 923–930. <https://doi.org/10.1093/bioinformatics/btt656> (2014).
40. Robinson, M. D., McCarthy, D. J. & Smyth, G. K. edgeR: A Bioconductor package for differential expression analysis of digital gene expression data. *Bioinformatics* **26**, 139–140. <https://doi.org/10.1093/bioinformatics/btp616> (2009).
41. Gómez-Rubio, V. ggplot2 - elegant graphics for data analysis. *J. Stat. Softw.* **77**, 1–13. <https://doi.org/10.18637/jss.v077.b02> (2017).
42. Raivo Kolde. Pheatmap: Pretty heatmaps. (2015)

Acknowledgements

This study was funded by NIH Grant (to QJC) K08AI168567. It was performed in collaboration The Center for Genomics and Bioinformatics and the Immune Assessment core facilities at UCLA. We thank Alexander Hoffmann, Scott Filler, Alberto Yanez, and David Williams for their feedback and suggestions. We thank Hollie David for copyediting and administrative contributions.

Author contributions

Q.J.C., K.F., J.F., Z.M., S.K.M., and J.S. performed the experiments. Q.J.C., K.F., J.F. and Z.M. analyzed the data. Q.J.C. wrote the manuscript. K.F. and J.F. edited the manuscript, and all authors approved the final version. Q.J.C. conceived of and obtained funding for the study.

Competing interests

The authors declare no competing interests.

Additional information

Supplementary Information The online version contains supplementary material available at <https://doi.org/10.1038/s41598-024-51620-8>.

Correspondence and requests for materials should be addressed to Q.J.C.

Reprints and permissions information is available at www.nature.com/reprints.

Publisher's note Springer Nature remains neutral with regard to jurisdictional claims in published maps and institutional affiliations.



Open Access This article is licensed under a Creative Commons Attribution 4.0 International License, which permits use, sharing, adaptation, distribution and reproduction in any medium or format, as long as you give appropriate credit to the original author(s) and the source, provide a link to the Creative Commons licence, and indicate if changes were made. The images or other third party material in this article are included in the article's Creative Commons licence, unless indicated otherwise in a credit line to the material. If material is not included in the article's Creative Commons licence and your intended use is not permitted by statutory regulation or exceeds the permitted use, you will need to obtain permission directly from the copyright holder. To view a copy of this licence, visit <http://creativecommons.org/licenses/by/4.0/>.

© The Author(s) 2024